Polymer Chemistry

ROYAL SOCIETY OF CHEMISTRY

COMMUNICATION

View Article Online
View Journal | View Issue

Cite this: *Polym. Chem.*, 2020, **11**, 669

Received 12th August 2019,
Accepted 6th December 2019

DOI: 10.1039/c9py01213c

rsc.li/polymers

Surface-grafted polyacrylonitrile brushes with aggregation-induced emission properties†

Maciej Kopeć, *[a,b] Marcin Pikiel[a,c] and G. Julius Vancso [a]

Polyacrylonitrile (PAN) was synthesized and grafted from silicon wafers by copper-mediated photoinduced atom transfer radical polymerization (ATRP) using α-bromophenyl acetic acid-based initiators. Aggregation-induced photonic emission (AIE) was observed in well-defined, low molecular weight (M_n < 10k) bulk PAN as well as in thin (d < 15 nm), surface-grafted polymer brushes.

With the advent of reversible addition radical polymerization (RDRP), polymer brushes have become a powerful interface engineering platform to functionalize surfaces by grafting well-defined macromolecules of a variety of two- or three-dimensional substrates.[1–3] Among the countless applications of different types of surface-grafted polymers, photoluminescent brushes are particularly interesting as ultrathin emissive layers for organic electronics, light harvesting, photovoltaics or 'smart' surfaces.[4–12] However, to synthesize photoactive brushes by surface-initiated polymerizations, chromophores need to be introduced either as side groups, or as the polymer chain end group. This is usually realized by polymerizing chromophore-containing monomers,[2,6,12] or resorting to various post-polymerization modification procedures.[7–11]

Interestingly, Zhou *et al.* have recently reported aggregation-induced emission (AIE) in commercial polyacrylonitrile (PAN).[13] AIE is an unusual behaviour observed in certain chromophores (AIE-gens), most notably tetraphenylethene derivatives. These molecules, unlike traditional chromophores, exhibit photoluminescence upon aggregation either in solution or in the solid state, due to the restriction of intramolecular rotational and vibrational motion.[14,15] Polymers containing AIE-gens have recently emerged as a straightforward approach to introduce AIE properties in films, fibres, composites as well as more sophisticated polymer architectures.[16–18] Typically, atom transfer radical polymerization (ATRP) or reversible addition fragmentation transfer (RAFT) polymerization with AIE-gen-modified initiators[19–22] or monomers[23,24] are used to incorporate AIE-gens in the polymer chain.

However, PAN is a non-conjugated polymer, traditionally used as a precursor to acrylic fibres, carbon fibres and carbon nanomaterials,[25] and does not contain any typical AIE-gens. The AIE phenomenon observed in PAN-based systems was instead ascribed to clustering of the nitrile (cyano) groups and to overlapping of their π and lone pair electrons, resulting in rigidified conformations which in turn facilitated the emissive deactivation of the excited state.[13] Similar behaviour was also demonstrated in a few other non-conjugated polymers.[26–28]

Herein, we report the synthesis of ultrathin (<15 nm), surface-grafted PAN brushes with solid-state AIE properties. To date, PAN was only grafted from nanostructured silica,[29–34] and polymeric macroinitiators for molecular bottlebrushes,[35,36] with no reports on grafting from planar surfaces. Difficulties in grafting PAN arise from the fact that in ATRP the activity of the alkyl halide initiator needs to be higher than that of the monomer, in order to ensure uniform growth of all chains.[37,38] Acrylonitrile (AN) is the most active monomer in ATRP, and its activity is higher than that of α-bromoisobutyrate, an initiator of choice for surface-initiated ATRP (SI-ATRP).[2,3] This precludes efficient synthesis of PAN brushes, unless the so-called halogen exchange technique is employed.[25] Indeed, halogen exchange enabled synthesis of PAN-grafted silica and bottlebrushes, but it requires large amounts of copper catalyst (*i.e.* normal ATRP conditions).[29–36] In order to facilitate polymerization of AN under low-catalyst-concentration ATRP techniques, such as ARGET (activators regenerated by electron transfer),[39] ICAR (initiators for continuous activator regeneration)[40] or SARA (supplemental activator reducing agent),[41] more active initiators, namely 2-bromopropionitrile (BPN) or ethyl 2-bro-

[a]*Materials Science and Technology of Polymers, MESA+ Institute for Nanotechnology, University of Twente, 7500 AE Enschede, The Netherlands*
[b]*Department of Chemistry, University of Bath, Claverton Down, Bath BA2 7AY, UK. E-mail: mk2297@bath.ac.uk*
[c]*Faculty of Chemistry, Lodz University of Technology, Wroblewskiego 15, 93-590 Lodz, Poland*

†Electronic supplementary information (ESI) available. See DOI: 10.1039/c9py01213c

mophenyl acetate (EBPA) need to be employed. Recently, EBPA initiators were used in metal-free ATRP of AN,[42] as well as to improve the initiation efficiency in SI-ATRP of methyl methacrylate.[43]

We aimed at grafting PAN brushes by copper-mediated photoinduced ATRP, which uses light (UV or visible) to regenerate Cu(II) to Cu(I). As in other activator regeneration ATRP techniques, this allows to drastically reduce catalyst concentrations.[44–47] Furthermore, photoinduced RDRP techniques have recently gained widespread interest for the preparation of polymer brushes due to their simplicity, straightforward patterning, temporal control and partial oxygen tolerance.[6,48–53] Since PAN was not synthesized by photoinduced ATRP before, we first developed conditions for the controlled photopolymerization of AN in solution (Scheme 1). The reaction was initiated by α-bromophenyl acetic acid (BPAA) in the presence of 50–290 ppm (*vs.* monomer) of $CuBr_2$/tris(2-pyridylmethyl)amine (TPMA, in 1 : 3 ratio) catalyst under UV irradiation (λ = 365 nm) in DMSO. Linear first order kinetics and linear increase of molecular weight (MW) with monomer conversion were observed, showing little dependence of the polymerization rate on the catalyst loading (Fig. 1 and Table 1, entries 1–3). Gel permeation chromatography (GPC) revealed symmetrical peaks and narrow MW distributions, with dispersities decreasing throughout the reaction to stay below 1.20 (Fig. 1c and S1†). Since GPC with a refractive index (RI) detector and poly(methyl methacrylate) (PMMA) calibration standards is known to significantly overestimate molecular weight values of PAN,[25,39] M_n was determined by ^{1}H NMR. Data such obtained revealed very good agreement with the theoretical values (Table 1). Furthermore, the chain-end functionality (CEF) of the PAN obtained was estimated by ^{1}H NMR to 98%, confirming excellent control over the polymerization (see Fig. S2† for the details of M_n and CEF calculations).

PAN samples were investigated by fluorescence spectroscopy and microscopy. Blue emission with a maximum at 431 nm under UV excitation (λ_{ex} = 348 nm) was observed in DMF upon increasing the concentration of PAN from 1.25 × 10^{-3} M to 2 M (Fig. S3†). Additionally, solid-state fluorescence in as-precipitated powders and drop-cast films was evident (Fig. 1d), reflecting the report by Zhou *et al.* on commercial PAN samples (with MW = 85k–150k).[13] Apparently, the proposed clustering of the nitrile groups occurs also in well-defined, low-molecular weight (MW < 10k) polymers. Thus, the AIE properties seem to be an intrinsic feature of essentially any PAN sample, regardless of its MW and/or dispersity. We note however, that given the reports showing AIE in polymers with single AIE-gens per chain,[19,20,22] elucidation of the minimal molecular weight of PAN at which clustering occurs would be of great interest.

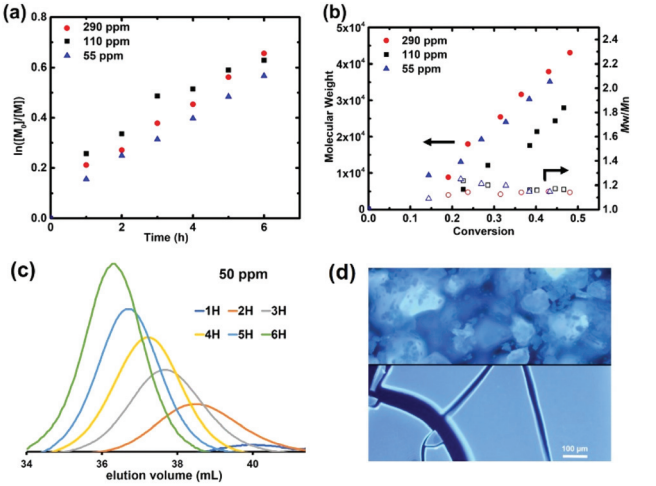

Fig. 1 (a) Semi-logarithmic first order kinetic plots and (b) molecular weight evolutions for photoinduced ATRP of acrylonitrile with different catalyst loadings. Reaction conditions: [AN] : [BPAA] : [$CuBr_2$] : [TPMA] = 500 : 1 : *n* : 3*n*; *n* = 0.025, 0.055 or 0.145, AN/DMSO = 1/2 (v/v), λ = 365 nm, rt, 6 h; (c) GPC traces for the reaction with 50 ppm of catalyst; (d) fluorescence microscopy images (λ_{ex} = 360 nm) of as-precipitated powder (top) and drop cast film (bottom) of the PAN synthesized ($M_{n,NMR}$ = 9100, Table 1, entry 3). Note that MWs in (b) are overestimated by PMMA calibration and thus theoretical lines are not shown.

Based on the above findings, we sought to explore if AIE could also occur in ultrathin, surface-grafted PAN films. In order to enable grafting of PAN by photoinduced ATRP, BPA-modified surfaces were prepared. Silicon wafers were first functionalized with 3-aminopropyltriethoxysilane (APTES) by chemical vapour deposition, followed by coupling of the amine groups with BPAA in the presence of EDC (*N*-(3-dimethylaminopropyl)-*N*′-ethylcarbodiimide hydrochloride, Fig. 2a). Successful functionalization was confirmed by the increase of the water contact angle from 60° to 73° (Fig. 2b and c).

As-prepared wafers were then used to graft PAN under similar conditions as described above for the bulk reactions. The reaction time was kept constant at 6 h, and the catalyst loading was set to 50, 200 or 400 ppm (*vs.* monomer) to modulate the rate of polymerization. After 6 h the wafers were analysed by FT-IR spectroscopy. The appearance of the C≡N stretching band centred at 2244 cm^{-1} evidenced that PAN was formed (Fig. 2d). As expected, its intensity increased with the concentration of the catalyst used, suggesting grafting of larger amounts of the polymer. Thicknesses of the films were determined by spectroscopic ellipsometry to be 4.2 nm, 9.4 nm and 14.5 nm for reactions conducted with 50, 200 and 400 ppm of the copper catalyst, respectively (Table 1, entries 4–6). This points to a stronger dependence of the polymerization rate on the catalyst concentration as compared with the bulk reac-

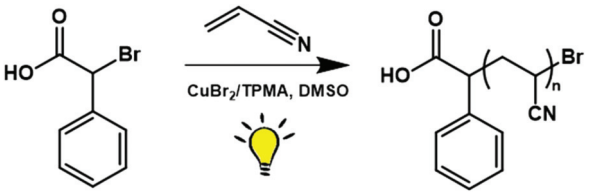

Scheme 1 Scheme of photoinduced ATRP of acrylonitrile.

Table 1 Results of bulk and surface-initiated polymerization of acrylonitrile by photoinduced ATRP

Entry[a]	Cu (ppm)	Conv.[b]	$M_{n,theo}$	$M_{n,GPC}$[c]	$M_{n,NMR}$	M_w/M_n	Thickness[d] (nm)
1	290	0.48	13 000	43 000	14 500	1.14	—
2	110	0.47	12 600	28 000	12 200	1.17	—
3[e]	50	0.43	10 300	35 000	9100	1.15	—
4	50	—	—	—	—	—	4.2 ± 0.0
5	200	—	—	—	—	—	9.4 ± 0.9
6	400	—	—	—	—	—	14.5 ± 1.2

[a] Entries 1–3: bulk polymerization, conditions: [AN] : [BPAA] : [$CuBr_2$] : [TPMA] = 500 : 1 : n : 3n; n = 0.025, 0.055 or 0.145, AN/DMSO = 1/2 (v/v), λ = 365 nm, rt, 6 h; entries 4–6: grafting from surfaces, conditions: AN/DMSO = 1/2 (v/v), V_0 = 3 mL, [$CuBr_2$/TPMA] = 50, 200 or 400 ppm (*vs.* AN), λ = 365 nm, rt, 6 h. [b] Determined by ^{1}H NMR in DMSO-d6. [c] Determined by GPC in DMF against linear PMMA calibration standards. [d] Determined by spectroscopic ellipsometry. [e] Targeted degree of polymerization = 442.

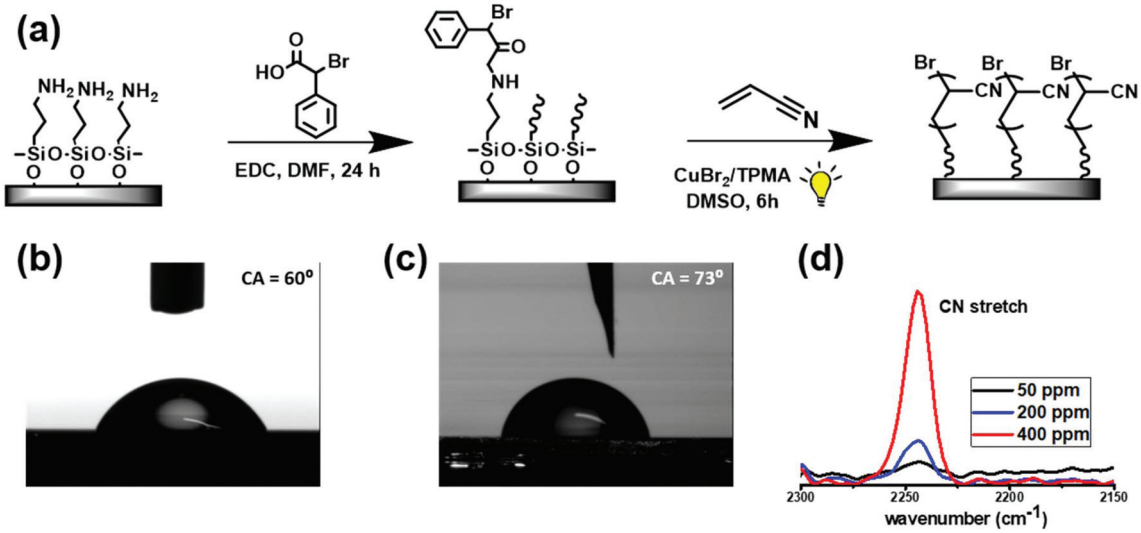

Fig. 2 (a) Schematic illustration of the synthetic route to PAN brushes by photoinduced SI-ATRP; water contact angle before (b) and after (c) coupling BPAA to the APTES-modified silicon wafer; (d) FT-IR spectra of the surface after SI-ATRP with different catalyst loadings.

tions. We note that no free polymer was detected in solution by NMR and precipitation tests, confirming that the polymerization occurred exclusively on the initiator-modified silicon surface.

Atomic force microscopy (AFM) observations of the films revealed uniform coverage of the surface with distinct submicron spherical domains (Fig. 3a–c). The root-mean-square surface roughness (R_q) measured by AFM increased from 2.2 nm to 4.8 nm with increasing film thickness, showing some discrepancy with the ellipsometric error (Table 1). However, these values are likely slightly overestimated due to the presence of larger aggregates visible in the AFM images.

The observed morphology of PAN aggregates on the surface could be due to local differences in grafting density caused by non-uniform initiator (and thus polymer) coverage, or by low initiation efficiency (slow initiation). However, a possibility of a specific organization of the grafted PAN chains cannot be ruled out. In bulk, PAN chains adopt a hexagonal structure driven by the dipole moments of the nitrile groups, which repel each other within one chain and form dipolar bonds between the chains.[25,41] These interactions make atactic PAN semi-crystalline and could influence the chain conformation within the densely grafted brushes. However, thorough examination of this morphology and its potential relationship with clustering of the CN groups is beyond the scope of the current communication.

Fluorescence microscopy of the grafted PAN (λ_{ex} = 348 nm) showed familiar blue colour, resembling images observed in bulk polymer films and powders. The emission was clearly visible from a remarkably large area, particularly in the sample grafted with 400 ppm of the catalyst and despite the film thickness of only around 15 nm (Fig. 3f). Plausibly, the same mechanism as observed before in bulk PAN and other non-conjugated polymers,[13,26–28] seems to also occur in thin PAN films. Namely, electron-rich, heteroatomic groups (*e.g.* nitrile or carbonyl) undergo clustering, further enhanced by the rigidification of clustered molecular assemblies. Such clusters effectively behave as chromophores and are responsible for the observed high energy/low wavelength (*i.e.* blue) emission. The detailed molecular mechanism underlying this so-called non-traditional intrinsic luminescence (NTIL) is still elusive, as very recently reviewed by Tomalia *et al.*[54]

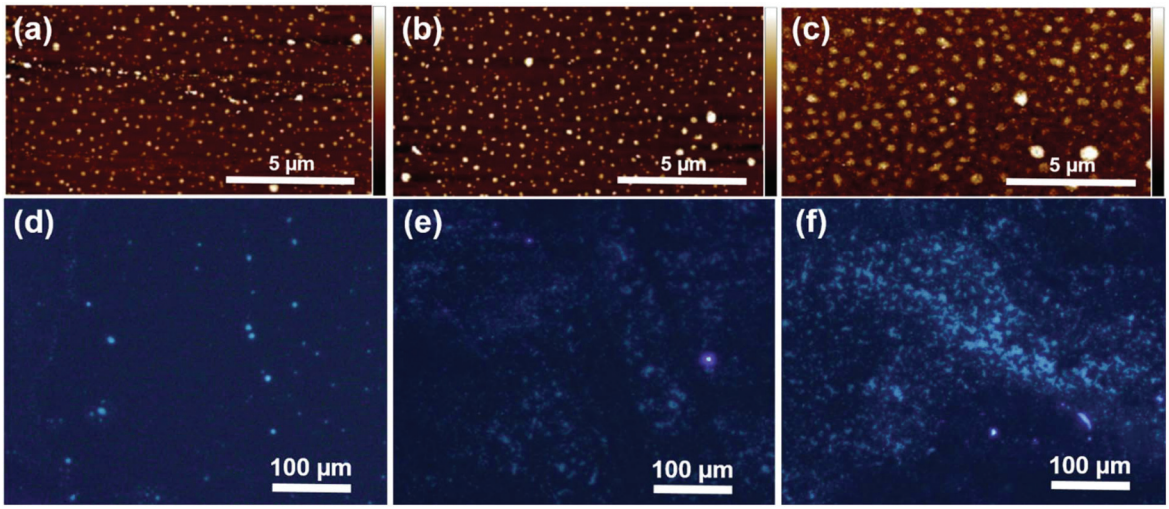

Fig. 3 AFM height images (a–c) and fluorescence microscopy images (d–f) of PAN brushes grafted from silicon substrates by photoinduced ATRP using 50 ppm (a, d), 200 ppm (b, e) and 400 ppm (c, f) of copper catalyst; *z*-scales are 20 nm, 15 nm and 35 nm in (a), (b), and (c), respectively.

In the case of surface-grafted polymers however, variations in grafting density could potentially lead to less aggregation and reduced emission. Even though a quantitative analysis of grafting densities was not possible due to the small thickness of the brushes, careful examination of the samples prepared with 50 ppm and 200 ppm of the catalyst seems to corroborate this notion. For the thinnest sample (d = 4.2 nm by ellipsometry, Fig. 3d), only several isolated fluorescent spots could be seen on the surface. Further growth of the brushes (d = 9.4 nm, Fig. 3e) lead to more uniform, interconnected emissive areas. Upon reaching $d \approx 15$ nm, the emission became more pronounced due to the formation of larger fluorescent clusters (Fig. 3f). Thus, the AIE behaviour likely develops with the film thickness, which in case of polymer brushes depends on grafting density and molecular weight of the grafted chains.[2] This suggest that AIE is suppressed in loosely packed chains, in analogy to dilute solutions in which PAN is not fluorescent.[13] Eventually, MW and grafting density become sufficient for clustering of the nitrile groups to occur, resulting in strong and more uniform emission from a large area. Such a gradual appearance of AIE points out to slow initiation, as suggested by AFM. On the contrary, the mechanism of AIE in PAN is still not clear, especially its dependence on MW.

In a control experiment, no fluorescence was recorded from a silicon wafer directly after deposition of APTES (Fig. S4†). We believe this is the first observation of AIE in such thin films and polymer brushes in particular. Furthermore, we have very recently shown that a collapse of stimuli-responsive PMMA brushes end-functionalized with fluorescein chromophores lead to aggregation and quenching of fluorescence.[9] In a striking contrast, the PAN brushes presented here are inherently luminescent in thin solid films due to the AIE phenomenon. Notably, these films are entirely composed of a commercially available polymer without any modification with photoactive moieties.

Conclusions

In summary, we grafted PAN from planar surfaces by employing photoinduced ATRP with ppm loadings of Cu catalyst. Solid-state AIE behaviour in surface-grafted PAN brushes was observed, and occurred likely due to the recently reported clustering of the nitrile groups. Since aggregation is an inherent feature of densely grafted polymer brushes, this study can open a way for the preparation of different surface-grafted systems exhibiting AIE. Additionally, the initial observation of AIE in low molecular weight, well-defined PAN can be extended to other polymer architectures, such as block copolymers, stars or molecular brushes. Intrinsic solid state fluorescence of such nanostructures can find application in optoelectronics, sensors, or smart surfaces. However, surface-initiated polymerization of acrylonitrile requires further optimization in order to prepare well-defined PAN brushes in a broad range of thickness and grafting density values. This will allow to separately analyse the effect of molecular weight and grafting density on the AIE properties in polymer brushes. Such studies are currently underway.

Conflicts of interest

There are no conflicts to declare.

Acknowledgements

MK and GJV thank the 4TU.High-Tech Materials research program: 'New Horizons in Designer Materials' for financial support. The authors are grateful to prof. Krzysztof Matyjaszewski for many fruitful comments and discussions.

References

1 C. M. Hui, J. Pietrasik, M. Schmitt, C. Mahoney, J. Choi, M. R. Bockstaller and K. Matyjaszewski, *Chem. Mater.*, 2014, **26**, 745–762.
2 J. O. Zoppe, N. C. Ataman, P. Mocny, J. Wang, J. Moraes and H.-A. Klok, *Chem. Rev.*, 2017, **117**, 1105–1318.
3 G. Xie, A. Khabibullin, J. Pietrasik, J. Yan and K. Matyjaszewski, Polymer Brushes by Atom Transfer Radical Polymerization, in *Polymer and Biopolymer Brushes: for Materials Science and Biotechnology*, ed. O. Azzaroni and I. Szleifer, John Wiley & Sons, Inc., Hoboken, NJ, USA, 2018, pp. 29–95.
4 O. Roling, K. De Bruycker, B. Vonhören, L. Stricker, M. Körsgen, H. F. Arlinghaus, B. J. Ravoo and F. E. Du Prez, *Angew. Chem., Int. Ed.*, 2015, **54**, 13126–13129.
5 K. Wolski, M. Szuwarzyński, M. Kopeć and S. Zapotoczny, *Eur. Polym. J.*, 2015, **65**, 155–170.
6 Z. A. Page, B. Narupai, C. W. Pester, R. Bou Zerdan, A. Sokolov, D. S. Laitar, S. Mukhopadhyay, S. Sprague, A. J. McGrath, J. W. Kramer, P. Trefonas and C. J. Hawker, *ACS Cent. Sci.*, 2017, **3**, 654–661.
7 M. Szuwarzyński, K. Wolski, A. Pomorska, T. Uchacz, A. Gut, Ł. Łapok and S. Zapotoczny, *Chem. – Eur. J.*, 2017, **23**, 11239–11243.
8 S. B. Jhaveri, M. Beinhoff, C. J. Hawker, K. R. Carter and D. Y. Sogah, *ACS Nano*, 2008, **2**, 719–727.
9 S. Tas, M. Kopeć, R. van der Pol, M. Cirelli, I. de Vries, D. A. Bölükbas, K. Tempelman, N. E. Benes, M. A. Hempenius, G. J. Vancso and S. de Beer, *Macromol. Chem. Phys.*, 2019, **220**, 1800537.
10 M. Kopeć, S. Tas, M. Cirelli, R. van der Pol, I. de Vries, G. J. Vancso and S. de Beer, *ACS Appl. Polym. Mater.*, 2019, **1**, 136–140.
11 N. Akkilic, R. Molenaar, M. M. A. E. Claessens, C. Blum and W. M. de Vos, *Langmuir*, 2016, **32**, 8803–8811.
12 H. J. Snaith, G. L. Whiting, B. Sun, N. C. Greenham, W. T. S. Huck and R. H. Friend, *Nano Lett.*, 2005, **5**, 1653–1657.
13 Q. Zhou, B. Cao, C. Zhu, S. Xu, Y. Gong, W. Z. Yuan and Y. Zhang, *Small*, 2016, **12**, 6586–6592.
14 Y. Hong, J. W. Y. Lam and B. Z. Tang, *Chem. Soc. Rev.*, 2011, **40**, 5361–5388.
15 Z. He, C. Ke and B. Z. Tang, *ACS Omega*, 2018, **3**, 3267–3277.
16 Z. Qiu, X. Liu, J. W. Y. Lam and B. Z. Tang, *Macromol. Rapid Commun.*, 2019, **40**, e1800568.
17 R. Hu, N. L. C. Leung and B. Z. Tang, *Chem. Soc. Rev.*, 2014, **43**, 4494–4562.
18 Y. B. Hu, J. W. Y. Lam and B. Z. Tang, *Chin. J. Polym. Sci.*, 2019, **37**, 289–301.
19 P.-Y. Gu, C.-J. Lu, F.-L. Ye, J.-F. Ge, Q.-F. Xu, Z.-J. Hu, N.-J. Li and J.-M. Lu, *Chem. Commun.*, 2012, **48**, 10234–10236.
20 P.-Y. Gu, Y.-H. Zhang, D.-Y. Chen, C.-J. Lu, F. Zhou, Q.-F. Xu and J.-M. Lu, *RSC Adv.*, 2015, **5**, 8167–8174.
21 R. Jiang, M. Liu, Q. Huang, H. Huang, Q. Wan, Y. Wen, J. Tian, Q.-y. Cao, X. Zhang and Y. Wei, *Polym. Chem.*, 2017, **8**, 7390–7399.
22 H. Wan, P. Gu, F. Zhou, H. Wang, J. Jiang, D. Chen, Q. Xu and J. Lu, *Polym. Chem.*, 2018, **9**, 3893–3899.
23 X. Zhang, X. Zhang, B. Yang, M. Liu, W. Liu, Y. Chen and Y. Wei, *Polym. Chem.*, 2014, **5**, 356–360.
24 X. Zhang, X. Zhang, B. Yang, J. Hui, M. Liu, Z. Chi, S. Liu, J. Xu and Y. Wei, *Polym. Chem.*, 2014, **5**, 683–688.
25 M. Kopeć, M. Lamson, R. Yuan, C. Tang, M. Kruk, M. Zhong, K. Matyjaszewski and T. Kowalewski, *Prog. Polym. Sci.*, 2019, **92**, 89–134.
26 L. Song, T. Zhu, L. Yuan, J. Zhou, Y. Zhang, Z. Wang and C. Tang, *Nat. Commun.*, 2019, **10**, 1315.
27 E. Zhao, J. W. Y. Lam, L. Meng, Y. Hong, H. Deng, G. Bai, X. Huang, J. Hao and B. Z. Tang, *Macromolecules*, 2015, **48**, 64–71.
28 H. Lu, L. Feng, S. Li, J. Zhang, H. Lu and S. Feng, *Macromolecules*, 2015, **48**, 476–482.
29 M. Kruk, B. Dufour, E. B. Celer, T. Kowalewski, M. Jaroniec and K. Matyjaszewski, *J. Phys. Chem. B*, 2005, **109**, 9216–9225.
30 M. Kruk, K. M. Kohlhaas, B. Dufour, E. B. Celer, M. Jaroniec, K. Matyjaszewski, R. S. Ruoff and T. Kowalewski, *Microporous Mesoporous Mater.*, 2007, **102**, 178–187.
31 M. Kruk, B. Dufour, E. B. Celer, T. Kowalewski, M. Jaroniec and K. Matyjaszewski, *Macromolecules*, 2008, **41**, 8584–8591.
32 C. Tang, L. Bombalski, M. Kruk, M. Jaroniec, K. Matyjaszewski and T. Kowalewski, *Adv. Mater.*, 2008, **20**, 1516–1522.
33 L. Cao and M. Kruk, *Polymer*, 2015, **72**, 356–360.
34 J. Zhang, Y. Song, Y. Zhao, S. Zhao, J. Yan, J. Lee, Z. Wang, S. Liu, R. Yuan, D. Luo, M. Kopeć, E. Gottlieb, T. Kowalewski, K. Matyjaszewski and M. R. Bockstaller, *Chem. Mater.*, 2018, **30**, 2208–2212.
35 C. Tang, B. Dufour, T. Kowalewski and K. Matyjaszewski, *Macromolecules*, 2007, **40**, 6199–6205.
36 R. Yuan, M. Kopeć, G. Xie, E. Gottlieb, J. W. Mohin, Z. Wang, M. Lamson, T. Kowalewski and K. Matyjaszewski, *Polymer*, 2017, **126**, 352–359.
37 W. Tang, Y. Kwak, W. Braunecker, N. V. Tsarevsky, M. L. Coote and K. Matyjaszewski, *J. Am. Chem. Soc.*, 2008, **130**, 10702–10713.
38 K. Matyjaszewski, *Macromolecules*, 2012, **45**, 4015–4039.
39 H. Dong, W. Tang and K. Matyjaszewski, *Macromolecules*, 2007, **40**, 2974–2977.
40 M. Lamson, M. Kopeć, H. Ding, M. Zhong and K. Matyjaszewski, *J. Polym. Sci., Part A: Polym. Chem.*, 2016, **54**, 1961–1968.
41 M. Kopeć, R. Yuan, E. Gottlieb, C. M. R. Abreu, Y. Song, Z. Wang, J. F. J. Coelho, K. Matyjaszewski and T. Kowalewski, *Macromolecules*, 2017, **50**, 2759–2767.
42 X. Pan, M. Lamson, J. Yan and K. Matyjaszewski, *ACS Macro Lett.*, 2015, **4**, 192–196.

43 J. Yan, X. Pan, M. Schmitt, Z. Wang, M. R. Bockstaller and K. Matyjaszewski, *ACS Macro Lett.*, 2016, **5**, 661–665.
44 M. Chen, M. Zhong and J. A. Johnson, *Chem. Rev.*, 2016, **116**, 10167–10211.
45 D. Konkolewicz, K. Schröder, J. Buback, S. Bernhard and K. Matyjaszewski, *ACS Macro Lett.*, 2012, **1**, 1219–1223.
46 X. Pan, M. A. Tasdelen, J. Laun, T. Junkers, Y. Yagci and K. Matyjaszewski, *Prog. Polym. Sci.*, 2016, **62**, 73–125.
47 N. Corrigan, J. Yeow, P. Judzewitsch, J. Xu and C. Boyer, *Angew. Chem., Int. Ed.*, 2019, **131**, 5224–5243.
48 J. E. Poelma, B. P. Fors, G. F. Meyers, J. W. Kramer and C. J. Hawker, *Angew. Chem., Int. Ed.*, 2013, **125**, 6982–6986.
49 E. H. Discekici, C. W. Pester, N. J. Treat, J. Lawrence, K. M. Mattson, B. Narupai, E. P. Toumayan, Y. Luo, A. J. McGrath, G. Clark, J. Read de Alaniz and C. J. Hawker, *ACS Macro Lett.*, 2016, **5**, 258–262.
50 M. Li, M. Fromel, D. Ranaweera, S. Rocha, C. Boyer and C. W. Pester, *ACS Macro Lett.*, 2019, **8**, 374–380.
51 E. M. Benetti, S. Zapotoczny and G. J. Vancso, *Adv. Mater.*, 2007, **19**, 268–271.
52 M. Vorobii, O. Pop-Georgievski, A. de los Santos Pereira, N. Y. Kostina, R. Jezorek, Z. Sedláková, V. Percec and C. Rodriguez-Emmenegger, *Polym. Chem.*, 2016, **7**, 6934–6945.
53 A. Bagheri, Z. Sadrearhami, N. N. M. Adnan, C. Boyer and M. Lim, *Polymer*, 2018, **151**, 6–14.
54 D. A. Tomalia, B. Klajnert-Maculewicz, K. A. M. Johnson, H. F. Brinkman, A. Janaszewska and D. M. Hedstrand, *Prog. Polym. Sci.*, 2019, **90**, 35–117.